

Layered oxychalcogenides: structural chemistry and thermoelectric properties

Article

Accepted Version

Creative Commons: Attribution-Noncommercial-No Derivative Works 4.0

Luu, S. D. N. and Vaqueiro, P. ORCID: <https://orcid.org/0000-0001-7545-6262> (2016) Layered oxychalcogenides: structural chemistry and thermoelectric properties. Journal of Materiomics, 2 (2). pp. 131-140. ISSN 2352-8478 doi: 10.1016/j.jmat.2016.04.002 Available at <https://centaur.reading.ac.uk/62768/>

It is advisable to refer to the publisher's version if you intend to cite from the work. See [Guidance on citing](#).

To link to this article DOI: <http://dx.doi.org/10.1016/j.jmat.2016.04.002>

Publisher: Elsevier

All outputs in CentAUR are protected by Intellectual Property Rights law, including copyright law. Copyright and IPR is retained by the creators or other copyright holders. Terms and conditions for use of this material are defined in the [End User Agreement](#).

www.reading.ac.uk/centaur

CentAUR

Central Archive at the University of Reading

Reading's research outputs online

Layered oxychalcogenides: structural chemistry and thermoelectric properties

Son D N Luu^{1,2}, Paz Vaqueiro^{2*}

¹Institute of Chemical Sciences, Heriot-Watt University, Edinburgh, EH14, 4AS, UK

²Department of Chemistry, University of Reading, Whiteknights, Reading, RG6 6AD, UK

Abstract

Layered oxychalcogenides have recently emerged as promising thermoelectric materials. The alternation of ionic oxide and covalent chalcogenide layers found in these materials often results in interesting electronic properties, and also facilitates the tuning of their properties via chemical substitution at both types of layers. This review highlights some common structure types found for layered oxychalcogenides and their interrelationships. This review pays special attention to the potential of these materials for thermoelectric applications, and provides an overview of the thermoelectric properties of materials of current interest, including BiCuSeO.

Keywords: Oxychalcogenides; Layered structures; Thermoelectric; BiCuSeO

* Corresponding author
E-mail: p.vaqueiro@reading.ac.uk

1. Introduction

Layered oxychalcogenides are mixed-anion compounds, in which oxide and chalcogenide anions (Group 16) indirectly bound via one or more cations, creating a stack of alternating oxide and chalcogenide layers. The coexistence of ionic oxide anions and more covalent chalcogenide anions leads to a highly distinctive structural chemistry. Owing to the preference of “hard” non-polarisable cations to coordinate to smaller oxide anions, while “soft” more polarisable cations preferentially coordinate to larger chalcogenide anions, quaternary oxychalcogenides tend to adopt structures in which oxide and chalcogenide anions are segregated, with each coordinating preferentially to one type of cation, as early noted by Guittard *et al* [1]. This often results in structures with low-dimensional characteristics, and structural low dimensionality may lead to highly anisotropic electronic band structures, together with interesting electronic properties. In addition, the covalent character of the chalcogenide layers promotes high-mobility semiconduction, whereas low thermal conductivity is favoured by the more ionic interactions of the oxide blocks. The alternation of distinct layers found in oxychalcogenides also facilitates the tuning of their properties via chemical substitution at both the oxide and chalcogenide layers. The coexistence of low-dimensionality together with covalent and ionic bonding offers great for potential for thermoelectric applications, and can also result in a wide range of unexpected and fascinating properties. For instance, $\text{Ce}_2\text{O}_2\text{S}$ nanoparticles anchored on graphitised carbon has been recently found to be a promising anode material for Li-ion batteries, with a stable specific capacity up to 627 mA h g^{-1} after 180 charge-recharge cycles [2]. $\text{Sm}_2\text{Ti}_2\text{S}_2\text{O}_5$ has attracted considerable attention as a photocatalyst for water splitting [3], and LaOCuS is considered a promising *p*-type transparent semiconductor for optoelectronic applications [4]. Superconductivity has been recently reported in bismuth oxysulfides, although the T_c is rather low $\sim 4.5 \text{ K}$ [5,6,7]. An improvement of the superconducting properties of compounds containing $[\text{BiS}_2]^{2-}$ layers has been found in electron doped $\text{NdO}_{0.5}\text{F}_{0.5}\text{BiS}_2$ ($T_c \sim 5 \text{ K}$) [8] or $\text{LaO}_{1-x}\text{F}_x\text{BiS}_2$ ($T_c \sim 10.6 \text{ K}$) [9].

Although oxychalcogenides can also adopt structures without low-dimensional characteristics, as exemplified by $\text{Eu}_5\text{V}_3\text{S}_6\text{O}_7$ and $\text{La}_{10}\text{Se}_{14}\text{O}$ [10], throughout this review we restrict our scope to layered oxychalcogenides, with a particular focus on their potential for thermoelectric applications. The structures of some families of layered oxychalcogenides have been previously reviewed [1, 11, 12].

2. Structural Chemistry of Layered Oxychalcogenides

2.1. Common Building Blocks

Structures of layered oxychalcogenides can be described as a combination of two (or more) types of building blocks. Certain inorganic slabs, such as perovskite, fluorite, or rock-salt blocks, which are encountered in many structures, can be considered as two-dimensional building blocks, and layered structures in which two or more types of such building blocks are stacked along a given direction, can be generated. **Table 1** presents four common building blocks found in layered oxychalcogenides. In each case, the parent structure is shown, as well as a two-dimensional slab derived from each parent structure. Representative compounds containing these building blocks are discussed in the following sections. Chalcogenide anions are denoted as Q.

2.2. Materials containing sheets of Q^{2-} and $(Q_2)^{2-}$ anions

Three related families of materials containing sheets of Q^{2-} and/or $(Q_2)^{2-}$ anions, which alternate with oxide slabs, are known. Planar sheets of Q^{2-} anions are found in $[A_2O_2]Q$, while $[A_4O_4](Q_2)(Q)$ contains both Q^{2-} and $(Q_2)^{2-}$, and in $[A_2O_2]Q_2$ only $(Q_2)^{2-}$ anions are present.

The crystal structures of materials with stoichiometry $[A_2O_2]Q$, where A is rare earth element (La-Yb, Y, Lu) or Bi, and Q is S, Se or Te, consist of alternating $[A_2O_2]^{2+}$ and Q^{2-} layers. The oxygen anions are tetrahedrally coordinated by A^{3+} cations, forming A_4O tetrahedra, while the Q^{2-} anions form a planar chalcogenide array. Two distinct structure types are found, which differ markedly on the nature of the $[A_2O_2]^{2+}$ layers. Materials containing the heavier chalcogen Te, including $[A_2O_2]Te$ (A = La-Nd, Sm-Ho Bi) [13,14] as well as the oxyselenide Bi_2O_2Se [15], crystallise in the tetragonal (space group $I4/mmm$) *anti*- $ThCr_2Si_2$ structure type (**Figure 1a**), while most of the remaining compounds ($[A_2O_2]Q$ with A = La-Yb, Y, Lu; Q = S, Se) [16,17,18,19] crystallise in the trigonal (space group $P\bar{3}m1$) structure (**Figure 1b**) of La_2O_3 . The structure of Bi_2O_2S , which is closely related to the *anti*- $ThCr_2Si_2$ type, has been described by Koyama *et al.* in an orthorhombic space group ($Pnmm$). This structure appears to be a slightly distorted form of the tetragonal structure of Bi_2O_2Se [20]. The *anti*- $ThCr_2Si_2$ structure is also adopted by the oxypnictides $[A_2O_2]X$ (A = rare-earth element, X= Sb, Bi) [21,22]. A commensurately modulated structure, arising from the distortion of the square nets of the pnictide ions, results in a lowering of the symmetry for Pr_2O_2Sb [23], but the single

crystal study of $\text{Bi}_2\text{O}_2\text{S}$ provides no evidence for a modulated structure [20].

In the tetragonal *anti*- ThCr_2Si_2 structure, the A_4O tetrahedra share four edges, forming fluorite-like two-dimensional slabs. The Q^{2-} ion adopts an 8-fold square prismatic coordination and the A site is in a (4O+4Q) distorted square anti-prism. By contrast, in the trigonal structure, the A_4O tetrahedra share three edges, forming 6 membered rings of tetrahedra (**Figure 1c**). Each chalcogenide ion is octahedrally coordination by A^{3+} cations, and each A^{3+} cation is seven coordinate with four short bonds to O and three longer bonds to Q.

In the $[\text{A}_4\text{O}_4](\text{Q}_2)(\text{Q})$ structure ($\text{A} = \text{La-Yb}$, Y and $\text{Q} = \text{Se}$), fluorite-like $[\text{A}_2\text{O}_2]^{2+}$ slabs alternate with chalcogen sheets, formed by chains of Se^{2-} and $(\text{Se}_2)^{2-}$ anions [24,25]. Depending on the size of the A atom, four closely-related structure types, labelled as the α , β , γ and δ - $\text{A}_4\text{O}_4\text{Se}_3$ structures, exist [23]. The structure of α - $\text{A}_4\text{O}_4\text{Se}_3$ phase is illustrated in **Figure 2a**. Whilst ordered chains of alternating Se^{2-} and $(\text{Se}_2)^{2-}$ anions are found in the α and β phases, in the γ and δ types the Se atoms form “wave like” chains, which cannot be interpreted as a simple ordered array of Se^{2-} and $(\text{Se}_2)^{2-}$. More details have been presented elsewhere [23]. Neither sulfur nor tellurium analogues of $\text{A}_4\text{O}_4\text{Se}_3$ have been reported to date.

The structure of $[\text{A}_2\text{O}_2](\text{Q}_2)$ (**Figure 2b**) was first described by Wichelhaus, who reported compounds where A is La, Pr, Nd and Q is S [26], and is composed of alternating fluorite-type $[\text{A}_2\text{O}_2]^{2+}$ layers and $(\text{S}_2)^{2-}$ planar sheets. Although this crystal structure was initially described in the *Pcam* space group [24], J. Ostoréro *et al.* have shown that $\text{La}_2\text{O}_2\text{S}_2$ crystallises in the *Cmca* space group [27]. Selenium or tellurium analogues have not been described.

2.3. Materials containing fluorite-like oxide blocks and transition-metal chalcogenide blocks

Two distinct structural types, both of which contain fluorite-like $[\text{A}_2\text{O}_2]^{2+}$ slabs, are known: $[\text{AO}][\text{BQ}]$ and $[\text{AO}][\text{BQ}_2]$, depending on the oxidation state of the transition metal. The monovalent transition metals Cu and Ag adopt the former, whilst divalent transition metals adopt the later structure.

Materials with the general formula $[\text{AO}][\text{BQ}]$ (where A is Bi, Y, La-Yb; B is a monovalent cation such as Cu, Ag and Q is S, Se, Te) [28,29,30,31,32], crystallise in the tetragonal ZrCuSiAs structure [33]. The A^{3+} ions had been limited to Y^{3+} and lanthanides until 1993

when Kholodkovskaya *et al.* [27] reported the substitution of Bi^{3+} into the A site. The $[\text{AO}][\text{BQ}]$ crystal structure consists of fluorite-type $[\text{A}_2\text{O}_2]^{2+}$ and antifluorite-type $[\text{B}_2\text{Q}_2]^{2-}$ slabs stacked alternately along the c -axis (Figure 3). This structure type has been reported for approximately 150 compounds, containing the anions oxide, fluoride, silicide, germanide, chalcogenide, pnictide, and hydride [34], and in particular, is also adopted by the superconducting oxypnictides LnOFePn ($\text{Ln} = \text{La, Pr, Ce, Sm}$; $\text{Pn} = \text{P and As}$) [35]. In 1980, Palazzi *et al.* reported ionic conductivity for LaOAgS [28], while in CeOCuS copper can be readily extracted from the $[\text{Cu}_2\text{S}_2]^{2-}$ layers, to produce highly deficient copper phases [36]. The rare-earth containing oxychalcogenides have been primarily investigated for their optoelectronic properties, as many of them are transparent p -type semiconductors [37].

The structure of $[\text{A}_2\text{O}_2][\text{BQ}_2]$ is composed of $[\text{BQ}_2]^{2-}$ ($\text{B} = \text{Fe, Zn, Mn, Cd}$; $\text{Q} = \text{Se}$) slabs separated by $[\text{A}_2\text{O}_2]^{2+}$ layers ($\text{A} = \text{La, Ce}$). In the chalcogenide layers, the B^{2+} cations occupy half of the available B sites of the antifluorite-type $[\text{B}_2\text{Q}_2]$ slab in an ordered fashion. In the case of $\text{La}_2\text{O}_2\text{CdSe}_2$, a checkerboard arrangement of corner-sharing CdSe_4 tetrahedra is found, instead of the edge-sharing tetrahedra found in $[\text{AO}][\text{BQ}]$ (**Figure 4**) [38]. It has been shown that different ordering patterns are possible depending on the composition, and in particular on the nature of the transition metal. The $[\text{BSe}_2]^{2-}$ layers can contain BSe_4 tetrahedra that are exclusively edge-sharing (stripe-like), exclusively corner-sharing (checkerboard-like arrangement), or mixtures of both. Details of the different ordering patterns in $[\text{A}_2\text{O}_2][\text{BSe}_2]$ phases have been discussed in detail elsewhere [39, 40]. The investigation of the electronic properties of $\text{La}_2\text{O}_2\text{CdSe}_2$ indicate that this material is insulating, with electrical resistivities $>10^{10} \Omega\text{cm}$, and a band gap of 3.3 eV [36].

2.4. Materials adopting the $[\text{AO}][\text{BQ}_2]$ structure and related structures

The repetition of fluorite-type $[\text{A}_2\text{O}_2]^{2+}$ blocks and rock-salt $[\text{B}_2\text{Q}_4]^{2-}$ blocks, stacked in an alternating fashion along the c -axis, creates the layered structure of $[\text{AO}][\text{BQ}_2]$ (where $\text{A} = \text{La, Ce, Pr, Nd, Sm, Yb, Bi}$; $\text{B} = \text{Bi}$; $\text{Q} = \text{S, Se}$), [41] which is exemplified by LaOBiS_2 (**Figure 5a**). These materials are currently attracting considerable attention due to their superconducting behavior and have been recently reviewed, [11] hence they will not be discussed here in further detail. $[\text{A}_2\text{O}_2][\text{SnS}_3]$ ($\text{A} = \text{La-Nd}$) can be considered to be closely related to the $[\text{AO}][\text{BQ}_2]$ structure, as it contains fluorite $[\text{A}_2\text{O}_2]^{2+}$ blocks alternating with thinner and distorted rock-salt $[\text{SnS}_3]^{2-}$ blocks [1, 42] (**Figure 5b**).

2.5. Materials adopting the $[A_2MO_2][B_2Q_2]$ structure and anti-type variants

A representative compound of the $[A_2MO_2][B_2Q_2]$ structure ($A = \text{Ba, Sr}$; $M = \text{Mn, Co, Ni, Zn}$; $B = \text{Cu, Ag}$; $Q = \text{S, Se}$) [43,44,45] is $\text{Sr}_2\text{ZnO}_2\text{Cu}_2\text{S}_2$ [46], which crystallises in the $\text{Sr}_2\text{Mn}_3\text{Sb}_2\text{O}_2$ (or $\text{Sr}_2\text{MnO}_2\text{Mn}_2\text{Sb}_2$) structure type [47]. This structure contains antifluorite $[B_2Q_2]^{2-}$ chalcogenide layers and oxide $[MO_2]^{2-}$ planar sheets, which are separated from the $[B_2Q_2]^{2-}$ blocks by A^{2+} ions (**Figure 6**). The $[A_2MO_2]^{2+}$ blocks can be considered to be derived from the perovskite structure, through removal of the apical oxide anions in a perovskite block (**Table 1**), leading to the square planar coordination found for the M^{2+} cations.

The $[A_2M_2O][B_2Q_2]$ structure is a half anti-type of $[A_2MO_2][B_2Q_2]$ in which A and M are monovalent cations. It comprises the same antifluorite chalcogenide layers $[B_2Q_2]^{2-}$ and oxide M_2O planar sheets, which are separated from the $[B_2Q_2]^{2-}$ slabs by A^+ ions. A representative compound is $\text{Na}_2\text{Cu}_4\text{OSe}_2$ or $[\text{Na}_2\text{OCu}_2][\text{Cu}_2\text{Se}_2]$, which exhibits p -type metallic behaviour due to a small sodium deficiency [48]. $[A_2O_2][B_2OQ_2]$ is an anti-structure of $[A_2M_2O][B_2Q_2]$. The representative compound of this structure type is $\text{La}_2\text{Fe}_2\text{O}_3\text{Se}_2$ or $[\text{La}_2\text{O}_2][\text{Fe}_2\text{OSe}_2]$ [49]. It consists of oxide fluorite-type slabs $[A_2O_2]^{2+}$, while the oxide M_2O planar sheet is separated from the $[A_2O_2]^{2+}$ layers by chalcogenide anions.

2.6. Materials containing Thicker Oxide Layers

Examples of materials containing thicker oxide layers include the following homologous series: $[A_{n+1}M_nO_{3n-1}][B_2Q_2]$ and $[A_{n+1}O_{2n}][B_2Q_2]$ ($n \geq 1$), in which B is Cu or Ag and Q is a chalcogen.

The structure of $[A_{n+1}M_nO_{3n-1}][B_2Q_2]$ ($A = \text{divalent cation}$; $M = \text{di- or trivalent}$; $Q = \text{S, Se}$) consists of antifluorite $[B_2Q_2]^{2-}$ layers alternating with perovskite-like $[A_{n+1}M_nO_{3n-1}]^{2+}$ slabs of different thicknesses (**Figure 7**). The structure for $n = 1$, $[A_2MO_2][B_2Q_2]$ (**Figure 6**), has been already described in section 2.5, and is exemplified by $\text{Sr}_2\text{ZnO}_2\text{Cu}_2\text{S}_2$. For $n = 2$, $[\text{Sr}_3\text{M}_2\text{O}_5][\text{Cu}_2\text{S}_2]$ with $M = \text{Fe}$ and Sc have been reported [43,50], while for $n = 3$ $[\text{Sr}_4\text{Mn}_3\text{O}_{7.5}][\text{Cu}_2\text{Q}_2]$ is known [51].

In the homologous series $[A_{n+1}O_{2n}][B_2Q_2]$, antifluorite-type $[Cu_2Q_2]$ layers are separated by fluorite-like $[A_{n+1}O_{2n}]$ oxide layers, in which A are trivalent cations (Bi, Y, La-Yb). The $n = 1$ member of this series, for which a representative example is $[\text{Bi}_2\text{O}_2][\text{Cu}_2\text{Se}_2]$ (or BiOCuSe),

has already been described in section 2.3. The $n=2$ members $[\text{Bi}_2\text{LnO}_4][\text{Cu}_2\text{Se}_2]$ ($\text{Ln} = \text{Y}, \text{Gd}, \text{Sm}, \text{Nd}, \text{La}$) are known [52], but members with higher values of n have not been reported to date.

2.7. Materials containing Thicker Chalcogenide Layers

Homologous series containing thicker chalcogenide layers have been primarily investigated for transition metals, and are exemplified by the $[\text{A}_2\text{MO}_2][\text{B}_{2n-\delta}\text{Q}_{n+1}]$ series ($\text{A} = \text{Ba}, \text{Sr}$; $\text{M} = \text{Mn}, \text{Co}, \text{Ni}, \text{Zn}$; $\text{B} = \text{Cu}, \text{Ag}$; $\text{Q} = \text{S}, \text{Se}$) [53]. The $n=1$ member of this series was already described in section 2.5, while $n=2$ and 3 members have been found, for instance, in $\text{Sr}_2\text{MnO}_2\text{Cu}_{2n-\delta}\text{S}_{n+1}$ [52]. As illustrated in **Figure 8**, members of this homologous series consist of perovskite-like $[\text{A}_2\text{MO}_2]$ blocks alternating with antifluorite-like $[\text{B}_{2n-\delta}\text{Q}_{n+1}]$ layers of increasing thickness depending on the value of n . Intergrowth structures in which antifluorite-like $[\text{B}_{2n-\delta}\text{Q}_{n+1}]$ blocks with different values of n coexist have also been found, as illustrated by $\text{Sr}_4\text{Mn}_2\text{Cu}_5\text{O}_4\text{S}_5$, which contains $[\text{Cu}_4\text{S}_3]$ and $[\text{Cu}_2\text{S}_2]$ layers [54]. It has been shown that in $\text{Sr}_2\text{MnO}_2\text{Cu}_{2n-\delta}\text{S}_{n+1}$ the copper ions can be replaced by lithium ions through topotactic ion exchange reactions [55].

3. Thermoelectric Properties of Oxychalcogenides

Despite the numerous families of oxychalcogenides that have been discovered, many of the published reports are concerned with their optical and magnetic properties [12, 36]. Little effort has been devoted to the study of their thermoelectric properties, the exception being the copper-containing oxyselenide BiOCuSe , which has been extensively investigated as a promising thermoelectric material since 2010 [56]. Some representative examples of thermoelectric oxychalcogenides are given in **Table 2**, and their properties are discussed below. As evidenced by data in **Table 2**, a common characteristic of these materials is a rather low thermal conductivity.

The first report of the thermoelectric performance of oxychalcogenides adopting the $[\text{AO}][\text{BQ}]$ structure focused on $\text{La}_{1-x}\text{Sr}_x\text{OCuSe}$ [57], but interest in these materials grew considerably after the report of $ZT = 0.76$ at 873 K for the bismuth analogue, $\text{Bi}_{1-x}\text{Sr}_x\text{OCuSe}$ [58]. Since then, the number of publications on this family of oxychalcogenides has been increasing steadily. Higher ZT values are found for oxychalcogenides with smaller band gaps. Usually, the temperature at which ZT reaches a maximum value is related to the band gap [59]. This is because for a given band gap energy, there is a temperature at which the onset of intrinsic

conduction will occur, and the simultaneous excitation of intrinsic electrons and holes will reduce the Seebeck coefficient ($S = S_p + S_n$) and hence ZT . It has been shown that, for a given operating temperature T , the optimal thermoelectric performance will be found for semiconductors with a band gap of approximately $10k_B T$ [60]. Bismuth-containing [AO][BQ] phases have significantly lower band gaps than those containing rare earth elements, due to the contribution of Bi $6p$ states to the bottom of the conduction band [61]. Although the lowest band gap is found for the oxytelluride for which $ZT = 0.66$ at 673 K, there is a very limited number of doping studies [62,63], and most of the effort in optimising the thermoelectric performance has centred on the bismuth oxyselenide. For instance, high values of the thermoelectric figure of merit, ZT , have been obtained by doping with divalent (Sr^{2+} , Ca^{2+} , Pb^{2+} , Mg^{2+}) [58,64,65,66] or monovalent cations (Na^+ , K^+) [67,68]. Alternatively, p -type doping can be achieved by introducing vacancies at the copper site, which leads to a ZT value of 0.81 at 923 K for $BiOCu_{0.975}Se$ [69]. In addition, the thermal conductivity of Ba^{2+} doped $BiOCuSe$ could be decreased by approximately 40% when reducing the grain sizes down to 200 - 400 nm, resulting in an even higher ZT value of 1.1 at 923 K [70]. Similar reductions in thermal conductivity have been found for ball milled $BiOCuSe$ [71], suggesting that nanostructuring may be an effective approach to enhance the thermoelectric response of these materials. The highest figure of merit, $ZT \sim 1.4$ (at 923 K), seems to have been achieved through the introduction of texture in $Bi_{0.875}Ba_{0.125}CuSeO$ by hot forging [72]. More recently, dual vacancies at the bismuth and the copper site have been exploited to reduce the thermal conductivity and control the charge carrier concentration, leading to a ZT value of 0.84 at only 750 K [73]. In general, the most common approach to achieve a high ZT in these oxychalcogenides is to tune the electrical conductivity via doping, given their naturally low thermal conductivity. Due to the high Grüneisen parameter of $BiOCuSe$ [74], it has been suggested that the low thermal conductivity in $BiOCuQ$ is related to the presence of the Bi^{3+} lone pair, which can reduce the lattice thermal conductivity due to bond anharmonicity [75]. Saha calculated the phonon band structure of the oxyselenide, and attributed the low thermal conductivity of $BiOCuSe$ when compared to $LaOCuSe$ to a stronger hybridization of acoustic and optical phonons in the former than in the later [76]. The origin of the unusual thermal transport properties of $BiOCuQ$ has also been investigated using a combination of neutron diffraction and computational calculations [77]. This study has shown that the main contributors to the unusually large Grüneisen parameter of these phases are copper and the chalcogen, and that despite the presence of the lone pair, the bismuth contribution is relatively small, with the change in thermal conductivity associated with the Bi/La substitution related to

the variation in atomic mass. Vaqueiro *et al.* concluded that weak bonding of the copper atoms leads to an unexpected rattling vibrational mode of copper at low frequencies, which is likely to be a major contributor to the low thermal conductivity found for BiOCuQ [76]. Recent calculations of phonon transport and lifetimes in BiOCuSe indicate that there is a significant contribution of optical phonons, arising primarily from O vibrations, to the overall lattice thermal conductivity [78]. Calculations of the electronic band structure of BiOCuQ indicate that the top of the valence band consist of a mixture of light- and heavy-mass bands [79]. This is considered a desirable feature for good thermoelectric performance [80], given that a light-mass band promotes good electrical conduction, whilst a heavy-mass band can result in a high Seebeck coefficient. However, it should be noted that the hole mobility in BiOCuSe is small, $\sim 20 \text{ cm}^2 \text{ V}^{-1} \text{ s}^{-1}$ [81]. This is detrimental for the thermoelectric performance, because ZT is proportional to the mobility, according to the expression $Z \propto (m^*)^{3/2} \mu$ (where m^* is the effective mass and μ the mobility)[59].

Other materials containing antifluorite-like $[\text{Cu}_2\text{Q}_2]$ layers have also been considered as potential thermoelectric materials. This includes $\text{Bi}_2\text{YO}_4\text{Cu}_2\text{Se}_2$, which was described in section 2.6. In $\text{Bi}_2\text{YO}_4\text{Cu}_2\text{Se}_2$, copper has a nominal oxidation state of +1.5 instead of +1.0, as confirmed by X-ray absorption spectroscopy [82], and this results in metallic behaviour. The large charge carrier density associated with metallic conduction leads to a significantly reduced Seebeck coefficient ($\sim 25 \text{ } \mu\text{VK}^{-1}$ at room temperature), and a ZT value of only 0.03 at 673 K [83]. A small number of materials consisting of antifluorite $[\text{Cu}_2\text{Se}_2]^{2-}$ layers alternating with perovskite-type oxide layers have also been assessed as potential thermoelectric materials. This includes $\text{A}_2\text{FeO}_3\text{CuQ}$ ($\text{A} = \text{Sr}, \text{Ca}$, $\text{Q} = \text{S}, \text{Se}$) [84] and $\text{Sr}_{2-x}\text{Ba}_x\text{CoO}_2\text{Cu}_2\text{Se}_2$ [85]. The $\text{A}_2\text{FeO}_3\text{CuQ}$ phases were found to be *p*-type semiconductors with high resistivity values of 1-10 k Ω cm at room temperature [76], while for $\text{Sr}_{2-x}\text{Ba}_x\text{CoO}_2\text{Cu}_2\text{Se}_2$ a power factor of 1.5 $\mu\text{W cm}^{-1}\text{K}^{-2}$ at room temperature has been reported [77]. The thermal conductivity of $\text{Sr}_{2-x}\text{Ba}_x\text{CoO}_2\text{Cu}_2\text{Se}_2$ has not been measured, but given that their hole mobility of $\sim 33.3 \text{ cm}^2 \text{ V}^{-1} \text{ s}^{-1}$ [42] is similar to that of BiOCuSe, doping studies of $\text{Sr}_2\text{CoO}_2\text{Cu}_2\text{Se}_2$, together with measurements of the thermoelectric properties as a function of temperature would be of interest, as these materials may exhibit good thermoelectric performance. There are also some preliminary studies of oxychalcogenides containing rock-salt blocks, including $\text{LaOBiS}_{2-x}\text{Se}_x$, for which a $ZT = 0.17$ is reached at 743 K [86]. More effort has been devoted to the thermoelectric properties of $\text{Bi}_2\text{O}_2\text{Q}$ ($\text{Q} = \text{Se}, \text{Te}$), which crystallise in the *anti*- ThCr_2Si_2 structure type described in section 2.2. The thermoelectric performance of $\text{Bi}_2\text{O}_2\text{Se}$, which is

an *n*-type semiconductor with a $ZT = 0.007$ at 300 K, was first reported by Ruleova *et al* [87]. Bismuth deficiency has been shown to improve ZT [88], whilst doping with Sn at the bismuth site in $\text{Bi}_{2-x}\text{Sn}_x\text{O}_2\text{Se}$ leads to a ZT value of 0.20 at 773 K [89]. The oxytelluride $\text{Bi}_2\text{O}_2\text{Te}$, which is a narrow gap semiconductor with a band gap of ~ 0.23 eV, reaches a value of 0.13 at 573 K [90]. As evidenced by the values of ZT presented in **Table 2**, the performance of *n*-type oxychalcogenides to date is significantly lower than those of *p*-type phases, and the best performing material is still BiOCuSe.

4. Concluding remarks

While in the past research on layered oxychalcogenides has centered on their magnetic properties, these materials are rapidly emerging as promising thermoelectric materials. A common feature to all materials investigated to date seems to be a relatively low thermal conductivity, and further studies to clarify the origin of this behavior are needed.

Band structure calculations suggest that the electronic structures of layered oxychalcogenides, which have a clear two-dimensional character, may be considered as the superposition of the electronic structures of each type of layer, stabilised by charge transfer. For the *p*-type phases containing $[\text{Cu}_2\text{Q}_2]$ blocks, the electrical transport properties will be primarily determined by the electronic structure of the $[\text{Cu}_2\text{Q}_2]$ layer, as the top of the valence band is formed by states arising from the hybridisation of Cu 3*d* and chalcogen *p* orbitals [30], while the oxide block acts as a charge reservoir to control the Fermi level. For the *n*-type oxychalcogenides, which have been far less investigated as thermoelectric materials, the electrical transport properties will be dependent on the nature of the bottom of the conduction band. For instance, in LaOBiS_2 , the bottom of the conduction band is formed by unoccupied Bi 6*p* states hybridized with S 3*p* states, and has a clear two-dimensional character, with conduction electrons located in the $[\text{BiS}_2]$ blocks [91].

From a thermoelectric perspective, the best performing oxychalcogenide to date is BiOCuSe, but given the variety of already known oxychalcogenides, there is a large field of unexplored materials that offer real prospects to improve ZT . The building block approach described here also offers ample opportunities to design and discover entirely new families of oxychalcogenides.

Acknowledgment

This work was funded by Energy Technology Partnership and European Thermodynamics

Ltd.

List of Figure Captions

Fig. 1. Crystal structures with stoichiometry $[A_2O_2]Q$: (a) *anti*- $ThCr_2Si_2$ type along $[010]$; (b) La_2O_3 type along $[100]$; (c) polyhedral view of the $[A_2O_2]^{2+}$ layer in the La_2O_3 type structure, with the OA_4 tetrahedra shown in blue. Unit cells are shown. Key: A, blue circles; O, red circles; Q, yellow circles.

Fig. 2. View of (a) the α - $A_4O_4Se_3$ crystal structure; (b) the $La_2O_2S_2$ structure. Key as for Figure 1.

Fig. 3. View of the crystal structure of $[AO][BQ]$ along $[010]$. Key: A, blue circles; B, green circles; O, red circles; Q, yellow circles.

Fig. 4. View of the crystal structure of $[AO][BQ_2]$ along $[010]$. Key as for Figure 2.

Fig. 5. View of the crystal structures of (a) $[AO][BQ_2]$ and (b) $[A_2O_2][SnS_3]$. Key as for Figure 2.

Fig. 6. The $[A_2MO_2][B_2Q_2]$ structure-type. Key: A, blue circles; B, green circles; M, pink circles; O, red circles; Q, yellow circles

Fig. 7. The $n=2$ and $n=3$ members of the homologous series $[A_{n+1}M_nO_{3n-1}][B_2Q_2]$. Key as for Figure 6.

Fig. 8. The $n=2$ and $n=3$ members of the homologous series $[A_2MO_2][B_{2n-6}Q_{n+1}]$. Key as for Figure 6.

Dr Paz Vaqueiro received a PhD in Chemistry from the University of Santiago de Compostela (Spain) and is currently a lecturer in Materials Chemistry at the University of Reading (UK). She previously held (2004-09) an EPSRC Advanced Research Fellowship for the investigation of high-performance thermoelectric materials. Her current research interests are focused on the solid-state chemistry and physics of thermoelectric materials, and since 2004, she has investigated the structure and properties of a wide range of materials, including skutterudites, transition-metal sulfides and oxychalcogenides. She is also involved in collaborative projects with engineering groups and industrial partners in the thermoelectric field.



Dr. Son D N Luu holds BSc, MSc degrees in Material Sciences and earned his PhD degree in Chemistry from Heriot-Watt University (2015). His research interests include materials for energy storage and conversion, gas sensing, nanostructuring and thin film materials for electronic applications. He is the author and co-author of 6 peer-reviewed papers.



Table 1. Common building blocks found in oxychalcogenides.

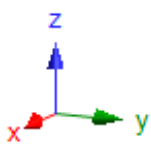
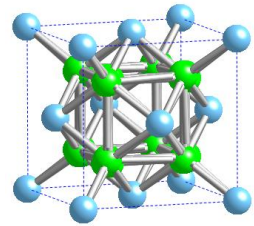
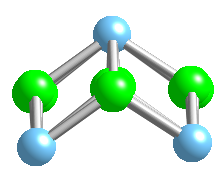

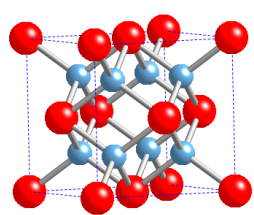
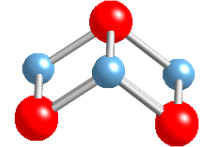
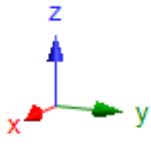
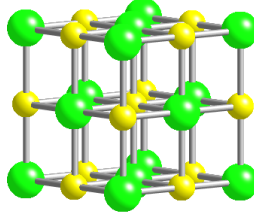
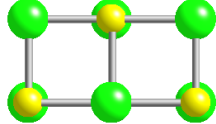
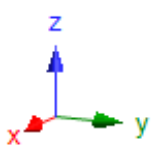
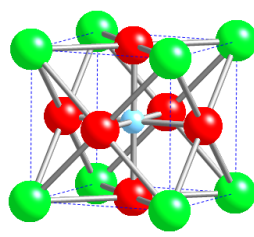
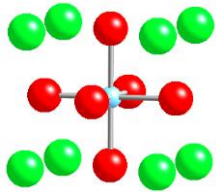
Structure	Unit cell	Building block slab	Key
Fluorite (CaF_2) 			Ca^{2+} (blue) F^- (green)
Antifluorite (Na_2O) 			Na^+ (blue) O^{2-} (red)
Rock-salt (NaCl) 			Na^+ (yellow) Cl^- (green)
Perovskite (SrTiO_3) 			Sr^{2+} (green) Ti^{4+} (blue) O^{2-} (red)

Table 2. Total thermal conductivity (at room temperature), together with maximum ZT values at a temperature T, for selected oxychalcogenides.

Material	<i>p/n</i> -type	$\kappa/\text{Wm}^{-1}\text{K}^{-1}$	ZT	T/K	Ref.
$\text{Bi}_{1-x}\text{Sr}_x\text{OCuSe}$	<i>p</i> -type	0.9	0.76	873	58
BiOCuTe	<i>p</i> -type	0.8	0.66	673	62
$\text{Bi}_{0.875}\text{Ba}_{0.125}\text{CuSeO}$	<i>p</i> -type	0.9	1.4	923	72
$\text{Bi}_2\text{YO}_4\text{Cu}_2\text{Se}_2$	<i>p</i> -type	1.5	0.03	673	83
$\text{LaOBiS}_{2-x}\text{Se}_x$	<i>n</i> -type	2.0	0.17	743	86
$\text{Bi}_{2-x}\text{Sn}_x\text{O}_2\text{Se}$	<i>n</i> -type	1.0	0.20	773	89
$\text{Bi}_2\text{O}_2\text{Te}$	<i>n</i> -type	0.9	0.13	573	90

References

- [1] M. Guittard, S. Benazeth, J. Dugue, S. Jaulmes, M. Palazzi, P. Laruelle, J. Flahaut, Oxysulfides and oxyselenides in sheets, formed by a rare earth element and a second metal, *J. Solid State Chem.* 51 (1984) 227-238.
- [2] J. Cheng, J. Zhu, X. Wei and P. K. Shen, Ce₂O₂S anchored on graphitized carbon with tunable architectures as a new promising anode for Li-ion batteries *J. Mater. Chem. A*, 3 (2015) 10026-10030.
- [3] A. Ishikawa, T. Takata, J. N. Kondo, M. Hara, H. Kobayashi, K. Domen, Oxysulfide Sm₂Ti₂S₂O₅ as a Stable Photocatalyst for Water Oxidation and Reduction under Visible Light Irradiation ($\lambda \leq 650$ nm) *J. Am. Chem. Soc.* 124 (2002) 13547–13553
- [4] K. Ueda, S. Inoue, S. Hirose, H. Kawazoe, H. Hosono, Transparent p-type semiconductor: LaCuOS layered oxysulfide, *Appl. Phys. Lett.* 77 (2000) 2701-2703.
- [5] S. K. Singh, A. Kumar, B. Gahtori, G. Sharma, S. Patnaik, and V.P. S. Awana, Bulk Superconductivity in Bismuth Oxysulfide Bi₄O₄S₃, *J. Am. Chem. Soc.* 134 (2012) 16504–16507.
- [6] Y. Mizuguchi, H. Fujihisa, Y. Gotoh, K. Suzuki, H. Usui, K. Kuroki, S. Demura, Y. Takano, H. Izawa, and O. Miura, BiS₂-based layered superconductor Bi₄O₄S₃ *Phys. Rev. B*. 86 (2012) 220510 (R).
- [7] W. A. Phelan, D. C. Wallace, K. E. Arpino, J. R. Neilson, K. J. Livi, C. R. Seabourne, A. J. Scott, T. M. McQueen, Stacking Variants and Superconductivity in the Bi–O–S System, *J. Am. Chem. Soc.* 135 (2013) 5372–5374.
- [8] R. Jha, A. Kumar, S. Kumar Singh, V.P.S. Awana, Superconductivity at 5 K in NdO_{0.5}F_{0.5}BiS₂ *J. Appl. Phys.*, 113 (2013) 056102.
- [9] Y. Mizuguchi, S. Demura, K. Deguchi, Y. Takano, H. Fujihisa, Y. Gotoh, H. Izawa, O. Miura, Superconductivity in Novel BiS₂-Based Layered Superconductor LaO_{1-x}F_xBiS₂ *J. Phys. Soc. Jpn.*, 81 (2012) 114725.
- [10] A. Meerschaut, A. Lafond, P. Palvadeau, C. Deudon, L. Cario, Synthesis and

crystal structure of two new oxychalcogenides: $\text{Eu}_5\text{V}_3\text{S}_6\text{O}_7$ and $\text{La}_{10}\text{Se}_{14}\text{O}$, *Mat. Res. Bull.* 37 (2002) 1895–1905.

[11] Y. Mizuguchi, Review of superconductivity in BiS_2 -based layered materials *J. Phys. Chem. Solids*, 84 (2015) 34-48.

[12] S. J. Clarke, P. Adamson, S. J. C. Herkelrath, O. J. Rutt, D. R. Parker, M. J. Pitcher, and C. F. Smura, Structures, Physical Properties, and Chemistry of Layered Oxychalcogenides and Oxypnictides *Inorg. Chem.* 47 (2008) 8473–8486.

[13] F.A. Weber, T. Schleid, On Oxytellurides ($\text{M}_2\text{O}_2\text{Te}$) of the Early Lanthanides ($\text{M} = \text{La-Nd}, \text{Sm-Ho}$) with A- or anti- ThCr_2Si_2 -Type Crystal Structure, *Z. Anorg. Allg. Chem.* 625 (1999) 1833-1838.

[14] S. D. N. Luu, P. Vaqueiro, Synthesis, characterisation and thermoelectric properties of the oxytelluride $\text{Bi}_2\text{O}_2\text{Te}$, *J. Solid State Chem.* 226 (2015) 219-223.

[15] H. Boller, Die Kristallstruktur von $\text{Bi}_2\text{O}_2\text{Se}$, *Monatsh. Chem.* 104 (1973) 916–919.

[16] H. A. Eick, The crystal structure and lattice parameters of some rare-earth mono seleno oxides, *Acta Crystallogr.*, 13 (1960) 161.

[17] M. Guittard, J. Flahaut, L. Domange, La série complète des oxysélénides des terres rares et d'yttrium, *Acta Crystallogr.*, 21 (1966) 832.

[18] W. H. Zachariasen, Crystal chemical studies of the 5f-series of elements. VII. The crystal structure of $\text{Ce}_2\text{O}_2\text{S}$, $\text{La}_2\text{O}_2\text{S}$ and $\text{Pu}_2\text{O}_2\text{S}$, *Acta Crystallogr.* 2 (1949) 60-62.

[19] H. A. Eick, The Preparation, Lattice Parameters and Some Chemical Properties of the Rare Earth Mono-thio Oxides, *J. Am. Chem. Soc.*, 80 (1958) 43–44.

[20] E. Koyama, I. Nakai, K. Nagashima, Crystal Chemistry of Oxide-Chalcogenides. II. Synthesis and Crystal Structure of the First Bismuth Oxide-Sulfide, $\text{Bi}_2\text{O}_2\text{S}$ *Acta Crystallogr., Sect. B*, 40 (1984) 105-109.

[21] R. Benz, $\text{Ce}_2\text{O}_2\text{Sb}$ and $\text{Ce}_2\text{O}_2\text{Bi}$ crystal structure *Acta Crystallogr. Section B* 27 (1971) 853–854.

[22] H. Mizoguchi, H. Hosono, A Metal–Insulator Transition in $\text{R}_2\text{O}_2\text{Bi}$ with an

Unusual Bi^{2-} Square Net (R = Rare Earth or Y) J. Am. Chem. Soc. 133 (2011) 2394–2397.

[23] O. V. Magdysyuk, J. Nuss, M. Jansen, Modulated crystal structure of Pr_2SbO_2 , Acta Cryst. B69 (2013) 547–555

[24] S. Strobel, A. Choudhury, P. K. Dorhout, C. Lipp and T. Schleid, Rare-Earth Metal(III) Oxide Selenides $\text{M}_4\text{O}_4\text{Se}[\text{Se}_2]$ (M = La, Ce, Pr, Nd, Sm) with Discrete Diselenide Units: Crystal Structures, Magnetic Frustration, and Other Properties Inorg. Chem., 47 (2008) 4936–4944.

[25] A. J. Tuxworth, C.-H. Wang, J. S. O. Evans, Synthesis, characterisation and properties of rare earth oxyselenides $\text{A}_4\text{O}_4\text{Se}_3$ (A = Eu, Gd, Tb, Dy, Ho, Er, Yb and Y), Dalton Trans. 44 (2015) 3009-3019.

[26] W. Wichelhaus, The rare-earth oxide disulfides $\text{La}_2\text{O}_2\text{S}_2$, $\text{Pr}_2\text{O}_2\text{S}_2$, and $\text{Nd}_2\text{O}_2\text{S}_2$ Naturwissenschaften, 65 (1978) 593-594.

[27] J. Ostorero, M. le Blanc, Room temperature structure of $\text{La}_2\text{O}_2\text{S}_2$ Acta Crystallogr, Sect. C, 46 (1990) 1376-1378.

[28] M. Palazzi, C. Carcaly and J. Flahaut, Un nouveau conducteur ionique $(\text{LaO})\text{AgS}$ J. Solid State Chem., 35 (1980) 150-155.

[29] G. H. Chan, B. Den, M. Bertoni, J.R. Ireland, M.C. Hersam, T.O. Mason, R.P. Van Duyne, J.A. Ibers, Syntheses, Structures, Physical Properties, and Theoretical Studies of CeM_xOS (M = Cu, Ag; $x \approx 0.8$) and CeAgOS , Inorg. Chem. 45 (2006) 8264-8272.

[30] B.A. Popovkin, A.M. Kusainova, V.A. Dolgikh, L.G. Aksel'rud, New Layered Phases of the MOCuX (M = Ln, Bi; X = S, Se, Te) Family: A Geometric Approach to the Explanation of Phase Stability, Russ. J. Inorg. Chem., 43 (1998) 1471–1475.

[31] L. N. Kholodkovskaya, L. G. Akselrud, A. M. Kusainova, V. A. Dolgikh and B. A. Popovkin, BiCuSeO : Synthesis and Crystal Structure, Mater. Sci. Forum., 133-136 (1993) 693-696.

[32] H. Hiramatsu, H. Yanagi, T. Kamiya, K. Ueda, M. Hirano, H. Hosono, Crystal

Structures, Optoelectronic Properties, and Electronic Structures of Layered Oxychalcogenides MCuOCh ($\text{M} = \text{Bi, La}$; $\text{Ch} = \text{S, Se, Te}$): Effects of Electronic Configurations of M^{3+} Ions, *Chem. Mater.* 20 (2008) 326-334.

[33] V. Johnson, W. Jeitschko, ZrCuSiAs : A “filled” PbFCl type, *J. Solid State Chem.* 11 (1974) 161-166.

[34] R. Pöttgen, D. Johrendt, Materials with ZrCuSiAs -type Structure, *Z. Naturforsch. B* 63 (2008) 1135–1148.

[35] S. Muir, M.A. Subramanian, ZrCuSiAs type layered oxypnictides: A bird's eye view of LnMPnO compositions, *Prog. Solid State Chem.* 40 (2012) 41–56.

[36] M. J. Pitcher, C. F. Smura, S. J. Clarke, Stoichiometric CeCuOS - A Well-Behaved Ce(III) Layered Oxysulfide, *Inorg. Chem.* 48 (2009) 9054–9056

[37] K. Ueda, H. Hiramatsu, M. Hirano, T. Kamiya, H. Hosono, Wide-gap layered oxychalcogenide semiconductors: Materials, electronic structures and optoelectronic properties, *Thin Solid Films*, 496 (2006) 8-15.

[38] H. Hiramatsu, K. Ueda, T. Kamiya, H. Ohta, M. Hirano and H. Hosono, Synthesis of single-phase layered oxychalcogenide $\text{La}_2\text{CdO}_2\text{Se}_2$: crystal structure, optical and electrical properties *J. Mater. Chem.* 14 (2004) 2946–2950.

[39] C-H. Wang, Ch.M. Ainsworth, D-Y. Gui, E. E. McCabe, M. G. Tucker, I. R. Evans, and J. S. O. Evans, Infinitely Adaptive Transition Metal Oxychalcogenides: The Modulated Structures of $\text{Ce}_2\text{O}_2\text{MnSe}_2$ and $(\text{Ce}_{0.78}\text{La}_{0.22})_2\text{O}_2\text{MnSe}_2$, *Chem. Mater.*, 27 (2015) 3121–3134.

[40] C. M. Ainsworth, C.-H. Wang, H. E. Johnston, E. E. McCabe, M. G. Tucker, H. E. A. Brand, and J. S. O. Evans, Infinitely Adaptive Transition-Metal Ordering in $\text{Ln}_2\text{O}_2\text{MSe}_2$ -Type Oxychalcogenides, *Inorg. Chem.* 54 (2015) 7230–7238.

[41] D. Yazici, I. Jeon, B.D. White, M. B. Maple, Superconductivity in layered BiS_2 -based compounds, *Physica C*, 514 (2015) 218–236.

[42] S. Bénazeth, M. Guittard et P. Laruelle, Structure de l'oxysulfure de lanthane et d'étain $(\text{LaO})_4\text{Sn}_2\text{S}_6$, *Acta Cryst. C* 41 (1985) 649-651.

- [43] S. Jin, X. Chen, J. Guo, M. Lei, J. Lin, J. Xi, W. Wang, W. Wang, $\text{Sr}_2\text{Mn}_3\text{Sb}_2\text{O}_2$ Type Oxyselenides: Structures, Magnetism, and Electronic Properties of $\text{Sr}_2\text{AO}_2\text{M}_2\text{Se}_2$ ($\text{A}=\text{Co}, \text{Mn}$; $\text{M}=\text{Cu}, \text{Ag}$), *Inorg. Chem.*, 51 (2012) 10185–10192.
- [44] K. Ottschi, H. Ogino, J. Shimoyama, K. Kishio, New candidates for superconductors; a series of layered oxysulfides $(\text{Cu}_2\text{S}_2)(\text{Sr}_{n+1}\text{M}_n\text{O}_{3n-1})$ *J. Low Temp. Phys.* 117 (1999) 729-733.
- [45] W. J. Zhu, P. H. Hor, A. J. Jacobson, G. Crisci, T. A. Albright, S. H. Wang, T. Vogt, $\text{A}_2\text{Cu}_2\text{CoO}_2\text{S}_2$ ($\text{A} = \text{Sr}, \text{Ba}$), a novel example of a square-planar CoO_2 layer *J. Am. Chem. Soc.* 119 (1997) 12398-12399.
- [46] W. J. Zhu, and P. H. Hor, Unusual Layered Transition-Metal Oxysulfides: $\text{Sr}_2\text{Cu}_2\text{MO}_2\text{S}_2$ ($\text{M} = \text{Mn}, \text{Zn}$) *J. Solid State Chem.* 130 (1997) 319-321.
- [47] E. Brechtel, G. Cordier, H. Schafer, On oxypnictides: preparation and crystal structure of $\text{A}_2\text{Mn}_3\text{B}_2\text{O}_2$ with $\text{A} = \text{Sr}, \text{Ba}$ and $\text{B} = \text{As}, \text{Sb}, \text{Bi}$, *Z. Naturforsch.*, 34b (1979) 777-780.
- [48] Y. B. Park, D. C. Degroot, J. L. Schindler, C. R. Kannewurf and M. G. Kanatzidis, Intergrowth of Two Different Layered Networks in the Metallic Copper Oxyselenide $\text{Na}_{1.9}\text{Cu}_2\text{Se}_2\cdot\text{Cu}_2\text{O}$, *Chem. Mater.*, 5 (1993) 8-10.
- [49] J. M. Mayer, L. F. Schneemeyer, T. Siegrist, J. V. Waszczak, B. Van Dover, New Layered Iron-Lanthanum-Oxide-Sulfide and -Selenide Phases: $\text{Fe}_2\text{La}_2\text{O}_3\text{E}_2$ ($\text{E} = \text{S}, \text{Se}$) *Angew. Chem. Int. Ed. Engl.*, 31 (1992) 1645-1647.
- [50] W. J. Zhu, P. H. Hor, Crystal Structure of New Layered Oxysulfides: $\text{Sr}_3\text{Cu}_2\text{Fe}_2\text{O}_5\text{S}_2$ and $\text{Sr}_2\text{CuMO}_3\text{S}$ ($\text{M} = \text{Cr}, \text{Fe}, \text{In}$) *J. Solid State Chem.*, 134 (1997) 128-131.
- [51] W. J. Zhu, P. H. Hor, Synthesis and Structure of Layered Manganese Oxychalcogenides: $\text{Sr}_2\text{CuMnO}_3\text{S}$ and $\text{Sr}_4\text{Cu}_2\text{Mn}_3\text{O}_{7.5}\text{Q}_2$ ($\text{Q} = \text{S}, \text{Se}$) *J. Solid State Chem.* 153 (2000) 26-29.
- [52] J. S. O. Evans, E. B. Brogden, A. L. Thompson, R. L. Cordiner, Synthesis and characterisation of the new oxyselenide $\text{Bi}_2\text{YO}_4\text{Cu}_2\text{Se}_2$, *Chem. Commun.* (2002)

912-913.

[53] Z. A. Ga'1, O. J. Rutt, C. F. Smura, T. P. Overton, N. Barrier, S. J. Clarke, J. Hadermann, Structural Chemistry and Metamagnetism of an Homologous Series of Layered Manganese Oxysulfides J. Am. Chem. Soc. 128 (2006) 8530-8540.

[54] N. Barrier, S. J. Clarke, A novel layered oxysulfide intergrowth compound $\text{Sr}_4\text{Mn}_2\text{Cu}_5\text{O}_4\text{S}_5$ containing a fragment of the $\alpha\text{-Cu}_2\text{S}$ antiferroite structure, Chem. Commun. (2003) 164-165.

[55] S. Indris, J. Cabana, O. J. Rutt, S. J. Clarke, C. P. Grey, Layered Oxysulfides $\text{Sr}_2\text{MnO}_2\text{Cu}_{2m-0.5}\text{S}_{m+1}$ ($m = 1, 2$, and 3) as Insertion Hosts for Li Ion Batteries J. Am. Chem. Soc. 128 (2006) 13354-13355.

[56] L-D. Zhao, J. He, D. Berardan, Y. Lin , J-F Li , C-W. Nan and N. Dragoe, BiCuSeO oxyselenides: new promising thermoelectric materials, Energy Environ. Sci., 7 (2014) 2900-2924.

[57] M. Yasukawa, K. Ueda, H. Hosono, Thermoelectric properties of layered oxyselenides $\text{La}_{1-x}\text{Sr}_x\text{CuOSe}$ ($x=0$ to 0.2) J. Appl. Phys. 95 (2004) 3594-3597.

[58]. L. D. Zhao, D. Berardan, Y. L. Pei, C. Byl, L. Pinsard-Gaudart, N. Dragoe, $\text{Bi}_{1-x}\text{Sr}_x\text{CuSeO}$ oxyselenides as promising thermoelectric materials App. Phys. Lett., 97 (2010) 092118.

[59] C. Wood, Materials for thermoelectric energy conversion, Rep. Prog. Phys. 51 (1988) 459-539.

[60] G. Mahan, B. Sales, J. Sharp, Thermoelectric materials: new approaches to an old problem, Phys. Today 50 (1997) 42.

[61] S. Sallis, L. F. J. Piper, J. Francis, J. Tate, H. Hiramatsu, T. Kamiya, H. Hosono, Role of lone pair electrons in determining the optoelectronic properties of BiCuOSe, Phys. Rev. B 85 (2012) 085207.

[62] P. Vaqueiro, G. Guélou, M. Stec, E. Guilmeau, A.V. Powell, A copper-containing oxytelluride as a promising thermoelectric material for waste heat recovery, J. Mater. Chem. A 1 (2013) 520-523.

- [63] T.-H. An, Y. S. Lim, H.-S. Choi, W.-S. Seo, C.-H. Park, G.-R. Kim, C. Park, C. H. Lee, J. H. Shim, Point defect-assisted doping mechanism and related thermoelectric transport properties in Pb-doped BiCuOTe, *J. Mater. Chem. A* 2 (2014) 19759-19764.
- [64] F. Li, T.-R. Wei, F. Kang, J.-F. Li, Enhanced thermoelectric performance of Ca-doped BiCuSeO in a wide temperature range, *J. Mater. Chem A*, 1 (2013) 11942-11949.
- [65] S. D. N. Luu, P. Vaqueiro, Synthesis, structural characterisation and thermoelectric properties of $\text{Bi}_{1-x}\text{Pb}_x\text{OCuSe}$, *J. Mater. Chem. A*, 1 (2013) 12270-12275.
- [66] J.-L. Lan, B. Zhan, Y.-C. Liu, B. Zheng, Y. Liu, Y.-H. Lin, C.-W. Nan, Doping for higher thermoelectric properties in p-type BiCuSeO oxyselenide, *Appl. Phys. Lett.*, 102 (2013) 123905-124100.
- [67] J. Li, J. Sui, Y. Pei, X. Meng, D. Berardan, N. Dragoe, W. Cai, L.-D. Zhao, The roles of Na doping in BiCuSeO oxyselenides as a thermoelectric material, *J. Mater. Chem. A*, 2 (2014) 4903-4906.
- [68] D.S. Lee, T. H. An, M. Jeong, H. S. Choi, Y. S. Lim, W. S. Seo, C. H. Park, C. Park, H. H. Park, Density of state effective mass and related charge transport properties in K-doped BiCuOSe, *Appl. Phys. Lett.*, 103 (2013) 232110.
- [69] Y. Liu, L.-D. Zhao, Y. Liu, J. Lan, W. Xu, F. Li, B.-P. Zhang, D. Berardan, N. Dragoe, Y.-H. Lin, C.-W. Nan, J.-F. Li, H. Zhu, Remarkable Enhancement in Thermoelectric Performance of BiCuSeO by Cu Deficiencies, *J. Am. Chem. Soc.* 133 (2011) 20112-20115.
- [70] J. Li, J. Sui, Y. Pei, C. Barreteau, D. Berardan, N. Dragoe, W. Cai, J. He and L.-D. Zhao, A high thermoelectric figure of merit $ZT > 1$ in Ba heavily doped BiCuSeO oxyselenides, *Energy Environ. Sci.* 5 (2012) 8543-8547.
- [71] F. Li, J.-F. Li, L. D. Zhao, K. Xiang, Y. Liu, B. P. Zhang, Y.-H. Lin, C.-W. Nan, H.-M. Zhu, Polycrystalline BiCuSeO oxide as a potential thermoelectric material, *Energy Environ. Sci.* 5 (2012) 7188-7195.

- [72] J. Sui, J. Li, J. He, Y.-L. Pei, D. Berardan, H. Wu, N. Dragoe, W. Cai and L.-D. Zhao, Texturation boosts the thermoelectric performance of BiCuSeO oxyselenides, *Energy Environ. Sci.* 6 (2013) 2916-2920.
- [73] Z. Li, C. Xiao, S. Fan, Y. Deng, W. Zhang, B. Ye, Y. Xie, Dual Vacancies: An Effective Strategy Realizing Synergistic Optimization of Thermoelectric Property in BiCuSeO, *J. Am. Chem. Soc.* 137 (2015) 6587-6593.
- [74] Y.-L. Pei, J. He, J.F. Li, F. Li, Q. Liu, W. Pan; C. Barreteau, D. Berardan, N. Dragoe, L.D. Zhao High thermoelectric performance of oxyselenides: intrinsically low thermal conductivity of Ca-doped BiCuSeO *NPG Asia Mater.* 5 (2013) e47.
- [75] M. D. Nielsen, V. Ozolins, J. P. Heremans, Lone pair electrons minimize lattice thermal conductivity, *Energy Environ. Sci.* 6 (2013) 570-578.
- [76] S.K. Saha, Exploring the origin of ultralow thermal conductivity in layered BiOCuSe *Phys. Rev. B* 92 (2015) 041202.
- [77] P. Vaqueiro, R. A. R. A. Orabi, Son D. N. Luu, G. Guélou, A. V. Powell, R. I. Smith, J.-P. Song, D. Wee, and M. Fornari, The Role of Copper in The Thermal Conductivity of Thermoelectric Oxychalcogenides: Do Lone Pairs Matter? *Phys. Chem. Chem. Phys.* 17 (2015) 31735–31740.
- [78] H. Shao, X. Tan, G.-Q. Liu, J. Jiang, H. Jiang, A first-principles study on the phonon transport in layered BiCuOSe *Sci. Rep.* 6 (2016) 21035.
- [79] D. Zou, S. Xie, Y. Liu, J. Lin, J. Li, Electronic structures and thermoelectric properties of layered BiCuOCh oxychalcogenides (Ch = S, Se and Te): first-principles calculations *J. Mater. Chem. A* 1 (2013) 8888-8896.
- [80] D.J. Singh, I.I. Mazin Calculated thermoelectric properties of La-filled skutterudites *Phys. Rev. B*, 56 (1997) R1650.
- [81] C. Barreteau, D. Bérardan, E. Amzallag, L.D. Zhao, N. Dragoe Structural and Electronic Transport Properties in Sr-Doped BiCuSeO *Chem. Mater.*, 24 (2012) 3168-3178.
- [82] T.-L. Chou, G. C. Tewari, T.-S. Chan, Y.-Y. Hsu, J.-M. Chen, H. Yamauchi, M.

Karppinen, Semiconducting BiOCuSe Thermoelectrics and Its Metallic Derivative Bi₂YO₄Cu₂Se₂, *Eur. J. Inorg. Chem.* (2015) 2574-2578.

[83] S. D. N. Luu, Synthesis and characterisation of oxychalcogenides as promising thermoelectric materials for waste heat recovery, PhD thesis, Heriot-Watt University, 2015.

[84] D. Berthebaud, O. I. Lebedev, D. Pelloquin, A. Maignan, Structural, magnetic and transport properties of 2D structured perovskite oxychalcogenides, *Solid State Sci.* 36 (2014) 94-100.

[85] T L Chou, O Mustonen, T S Tripathi, M Karppinen, Isovalent Ca and Ba substitutions in thermoelectric layer-structured oxyselenide Sr₂CoO₂Cu₂Se₂, *J. Phys.: Condens. Matter* 28 (2016) 035802.

[86] Y. Mizuguchi, A. Omachi, Y. Goto, Y. Kamihara, M. Matoba, T. Hiroi, J. Kajitani, O. Miura, Enhancement of thermoelectric properties by Se substitution in layered bismuth-chalcogenide LaOBiS_{2-x}Se_x, *J. Appl. Phys.* 116 (2014) 163915.

[87] P. Ruleova, C. Drasar, P. Losak, C.-P. Li, S. Ballikaya, C. Uher, Thermoelectric properties of Bi₂O₂Se, *Mater. Chem. Phys.* 119 (2010) 299-302.

[88] B. Zhan, Y. Liu, X. Tan, J.-L. Lan, Y.-H. Lin, C.-W. Nan, Enhanced Thermoelectric Properties of Bi₂O₂Se Ceramics by Bi Deficiencies, *J. Am. Ceram. Soc.* 98 (2015) 2465–2469.

[89] B. Zhan, S. Butt, Y. Liu, J.-L. Lan, C.-W. Nan, Y.-H. Lin, High-temperature thermoelectric behaviors of Sn-doped n-type Bi₂O₂Se ceramics, *J. Electroceram.* 34 (2015) 175-179.

[90] S. D. N. Luu, P. Vaqueiro, Synthesis, characterisation and thermoelectric properties of the oxytelluride Bi₂O₂Te, *J. Solid State Chem.* 226 (2015) 219-223.

[91] I. R. Shein, A. L. Ivanovskii, Electronic band structure and Fermi surface for new layered superconductor LaO_{0.5}F_{0.5}BiS₂ in comparison with parent phase LaOBiS₂ from first principles, *JETP Letters* 96 (2012) 769–774.